Published in final edited form as:

*J Cell Physiol*. 2016 May ; 231(5): 1130–1141. doi:10.1002/jcp.25210.

# The Nox1/4 dual inhibitor GKT137831 or Nox4 knockdown inhibits Angiotensin-II-induced adult mouse cardiac fibroblast proliferation and migration. AT1 physically associates with Nox4

**Naveen K. Somanna**[1], **Anthony J. Valente**[2], **Maike Krenz**[3], **William P. Fay**[4], **Patrice Delafontaine**[4], and **Bysani Chandrasekar**[4,5,*]

[1]Microbiology, Tulane University School of Medicine, New Orleans, LA 70112

[2]Medicine, University of Texas Health Science Center, San Antonio, TX 78229

[3]Department of Medical Pharmacology and Physiology, University of Missouri-Columbia, Columbia, MO 65211

[4]Medicine/Cardiology, University of Missouri, Columbia, MO 65212

[5]Research Service, Harry S. Truman Memorial Veterans Hospital, Columbia, MO 65201

## Abstract

Both oxidative stress and inflammation contribute to chronic hypertension-induced myocardial fibrosis and adverse cardiac remodeling. Here we investigated whether angiotensin (Ang)-II-induced fibroblast proliferation and migration are NADPH oxidase (Nox) 4/ROS and IL-18 dependent. Our results show that the potent induction of mouse cardiac fibroblast (CF) proliferation and migration by Ang-II is markedly attenuated by Nox4 knockdown and the Nox inhibitor DPI. Further, Nox4 knockdown and DPI pre-treatment attenuate Ang-II-induced IL-18, IL-18Rα and collagen expression, and MMP9 activation. While neutralization of IL-18 blunted Ang-II-induced CF proliferation and migration, knockdown of MMP9 attenuated CF migration. The antioxidant NAC and the cell-permeable SOD mimetics Tempol, MnTBAP, and MnTMPyP attenuated oxidative stress and inhibit CF proliferation and migration. The Nox1/Nox4 dual inhibitor GKT137831 also blunted Ang-II-induced $H_2O_2$ production and CF proliferation and migration. Further, AT1 binds Nox4, and Ang-II enhanced their physical association. Notably, GKT137831 attnuated the AT1/Nox4 interaction. These results indicate that Ang-II induces CF proliferation and migration in part via Nox4/ROS-dependent IL-18 induction and MMP9 activation, and may involve AT1/Nox4 physical association. Thus, either (i) neutralizing IL-18, (ii) blocking AT1/Nox4 interaction or (iii) use of the Nox1/Nox4 inhibitor GKT137831 may have therapeutic potential in chronic hypertension-induced adverse cardiac remodeling.

To whom correspondence should be addressed: Bysani Chandrasekar, DVM. Ph.D., Research Service, Harry S. Truman Memorial Veterans Hospital, 800 Hospital Drive, Columbia, MO 65201, Tel.: 573-882-2296, chandrasekarb@health.missouri.edu.

**Conflict of Interest**

None.

**Keywords**

Hypertension; adverse cardiac remodeling; fibrosis; migration; mitogenesis; Nox4

## Introduction

Persistent hypertension or a chronic increase in systemic angiotensin II (Ang-II) levels contributes to myocardial fibrosis and adverse remodeling (Gonzalez et al., 2004; McMaster et al., 2015). Cardiac fibroblasts (CF), the predominant cell type in the heart, play a major role in fibrosis (Chen and Frangogiannis, 2010; Kong et al., 2014). In the normal heart, fibroblasts remain quiescent and are responsible for basal deposition and degradation of extracellular matrix. However, under stressed conditions, such as chronic hypertension, fibroblasts differentiate into myofibroblasts that migrate and proliferate, and secrete higher levels of extracellular matrix components, resulting in fibrosis and contractile dysfunction (Iwata et al., 2011; Tsutsumi et al., 1998).

Matrix metalloproteinases (MMPs) play a pivotal role in ECM regulation. Under stress conditions, their enhanced activation promotes ECM degradation, and stimulates fibroblast migration and proliferation. CF express various MMPs, including the gelatinases MMP2 and MMP9. CF are also a rich source of cytokines, chemokines, and growth factors, biological substances with known positive effects on MMP2 and 9 expression, secretion, and activation (Chen and Frangogiannis, 2010; Kong et al., 2014). Interleukin (IL)-18 is a proinflammatory cytokine and an inducer of MMPs. IL-18 also exerts pro-mitogenic and pro-migratory effects in CF and aortic SMC (Fix et al., 2011; Siddesha et al., 2014; Valente et al., 2013). Increased expression of IL-18 in the heart results in myocardial hypertrophy and contractile dysfunction (Toldo et al., 2014; Yu et al., 2009). Targeting IL-18 secretion by neutralizing antibodies or IL-18BP, a natural IL-18 antagonist, blunts Ang-II and aldosterone-induced pro-fibrotic effects *in vitro* (Somanna et al., 2015; Valente et al., 2012). Importantly, oxidative stress induces IL-18 expression in CF.

Hypertensive heart disease (HHD) is characterized by sustained oxidative stress. It is known that Ang-II can induce oxidative stress by stimulating NADPH oxidase (Nox) activity and ROS generation. Among the 7 Nox/Duox family members, Nox4 is the predominant isoform expressed in CF (Colston et al., 2005). Nox4 is constitutively expressed and hydrogen peroxide is the usual measurable product of its activation (Takac et al., 2011). Another unique feature of Nox4 is that it does not require other cytosolic Nox components for its activation. Previously we reported that Ang-II induces cardiomyocyte hypertrophy in part via Nox2/superoxide (Shanmugam et al., 2011), and arterial smooth muscle cell proliferation via Nox1-dependent superoxide generation (Valente et al., 2012), and in both cases there was an increased association between the Nox proteins and the Ang-II receptor type I (AT1). Here we investigated whether Ang-II-induced fibroblast migration and proliferation are dependent on Nox4 and hydrogen peroxide production.

Our results indicate that Ang-II induces both migration and proliferation of primary adult mouse CF in part via Nox4. Knockdown of Nox4 or treatment with small molecule Nox1/Nox4 dual inhibitor GKT137831 (GKT) markedly attenuated Ang-II-induced hydrogen

peroxide production and CF migration and proliferation. These effects were mimicked by the antioxidant NAC and the SOD mimetics Tempol, MnTBAP, and MnTMPyP. Further, Ang-II induces Nox4/ROS-dependent IL-18 and IL-18Rα induction, collagen expression and secretion, and MMP9 and LOX activation. Neutralization of IL-18 blunted Ang-II-induced CF migration and proliferation, and silencing MMP9 attenuated CF migration. Moreover AT1 bound Nox4, and Ang-II, but not IL-18, enhanced their physical association. Notably, GKT attenuated their binding interaction. These results indicate that Ang-II induces CF proliferation and migration in part via Nox4/ROS-dependent IL-18 induction and MMP9 activation, and may involve AT1/Nox4 physical association. These results suggest that (i) neutralizing IL-18, (ii) blocking AT1/Nox4 interaction with small molecule inhibitors, or (iii) use of the Nox1/Nox4 dual inhibitor GKT137831 may have therapeutic potential in chronic hypertension-induced adverse cardiac remodeling.

## Materials and methods

### Materials

Human angiotensin II (Ang-II; # A9525), AT1 antagonist losartan potassium (#61188; 10 mM for 1 h), diphenyleneiodonium chloride (DPI; # D-2926; 10 μM in DMSO for 30 min), anti-β-actin antibody used in immunoblotting (#A5441), fluorescein isothiocyanate (FITC)-conjugated monoclonal anti-β-actin (#F3022) and smooth muscle actin (#F3777) used in fibroblast characterization, anti-MMP9 antibody (#M9570) that detects both pro and active forms, insulin-transferrin-sodium selenite (ITS) liquid media supplement (#I3146), 3-aminopropionitrile fumarate salt (BAPN; #A3134), N-acetyl-L-cysteine (NAC, 5mM in water for 30 min; #A7250), and all other chemicals were purchased from Sigma-Aldrich (St. Louis, MO). Anti-platelet-endothelial cell adhesion molecule-1 (PECAM-1 or CD-31; # 10R-CD31jMSP) antibodies used in fibroblast characterization were purchased from Fitzerald Industries International (Acton, MA). The Nox1/Nox4 inhibitor GKT137831 (2-2(chlorophenyl)-4-[3-(dimethylamino) phenyl]-5-methyl-1H-pyrazolo[4,3-c]pyridine-3,6(2H,5H)-dione; #17164), TBA malondialdehyde (MDA) Standard (#10009202), Thiobarbituric Acid Reactive Substances (TBARS) Assay kit (#700870) and Vybrant® MTT (3-(4,5-dimethylthiazol-2-yl)-2,5-diphenyltetrazolium bromide) Cell Proliferation Assay Kit (V13154) were purchased from Cayman Chemical (Ann Arbor, MI). Nox4 antibodies (#3187-1) used in immunprecipitation (IP) and immunoblotting (IB) were purchased from Epitomics (Burlingame, CA). AT1 antibodies (#sc-1173) used in IP and IB, anti-vimentin (#sc-373717) antibodies used in fibroblast characterization, and cell permeable superoxide dismutase (SOD) mimetics MnTBAP chloride (Manganese (III) tetrakis (4-benzoic acid) porphyrin chloride; CAS 55266-18-7; 100 μM in water) and MnTMPyP pentachloride (Manganese (III) tetrakis(1-methyl-4-pyridyl)porphyrin pentachloride; #sc-221956; 1 μM in water for 30 min) were from Santa Cruz Biotechnology, Inc. (Dallas, TX). IL-18 antibodies used in immunoblotting (D043–3), IL-18BP-Fc chimera (119-BP-100; 10 μg/ml for 1 h), and Fc (#100-HG) were purchased from R&D Systems (Minneapolis, MN). Antibodies against Akt (no. 9272), phospho-p65 (p-p65, Ser536; #3033), phospho-c-Jun (p-c-Jun, Ser73; #9261), gp130 (# 3732), MMP-9 (#3852S), and α-tubulin (#2144) were purchased from Cell Signaling Technology (Beverly, MA). IL-18Rα antibodies (223548) were from United States Biologicals (Salem, MA). Anti-lysyl oxidase

(LOX, #PA1-16953) antibodies, Restore™ Western blot Stripping Buffer (#21059), and Amplex® Red Hydrogen Peroxide/Peroxidase Assay Kit (#A22188) were from ThermoFisher Scientific (Grand Island, NY). Antibodies against collagen type 1 (#ab34170) and collagen type III (#ab7778) were from Abcam (Cambridge, MA). Anti-CTGF-1 (#210303) antibodies were from United States Biological (Salem, Massachusetts). MMP9 Biotrak activity assay (#RPN2634) was purchased from GE Healthcare Life Bio-Sciences (Pittsburg, PA). Tempol (1-oxyl-2,2,6,6-tetramethyl-4-hydroxypiperidine, #3082; 1 μM in DMSO), a membrane-permeable superoxide scavenger, was purchased from TOCRIS Bioscience (Ellisville, MO). Amicon Ultra-0.5 centrifugal filter unit with ultracel-10 membrane (#UFC501008), MMP9 proform (#AB19016), were from Millipore (Billerica, MA). Mouse IL-18 ELISA kit (#BMS618/2) was from Affymetrix eBioscience (San Diego, CA).

## Isolation and culture of adult mouse cardiac fibroblasts

This investigation conforms to the *Guide for the Care and Use of Laboratory Animals*, published by the National Institutes of Health (DRR/National Institutes of Health, 1996), and all protocols were approved by the Institutional Animal Care and Use Committee of Tulane University (New Orleans, LA). Cardiac fibroblasts (CF) were isolated from normotensive adult male C57Bl/6 mice (~3 m of age, ~25 g; The Jackson Laboratories) as previously described (Siddesha et al., 2014; Somanna et al., 2015). CF and non-fibroblast contaminants were identified by immunofluorescence (IF) using antibodies against β-actin, PECAM-1, vimentin, and smooth muscle actin. Around 99.6% of cells exhibited vimentin and β-actin immunoreactivity, were PECAM-1 and smooth muscle actin-negative, and displayed typical fibroblast-like morphology. Non-fibroblast cells typically account for <0.1% of total cells as determined by IF. CF were cultured in complete medium (RPMI 1640 medium with 5 mM glucose, 10% heat-inactivated FBS, and antibiotics; pH 7.3), and used in these experiments between passages 2–3. At 70% confluency, the cells were made quiescent by incubating in conditioning medium (RPMI 1640 [RPMI] medium with 5 mM glucose, 0.5% BSA, and antibiotics; pH 7.3) for 48 h. In studies investigating the effect of Ang-II on MMP9 activation, the conditioned media contained ITS supplement (1X) in place of 0.5% BSA. Similar to RPMI+0.5% BSA, the serum-free RPMI/ITS did not affect cell viability, shape or adherence to culture dishes. At the end of the experimental period, culture supernatants were collected and snap frozen. Cells were harvested, snap frozen, and stored at −80°C. Dimethyl sulfoxide (DMSO) was used to dissolve some of the pharmacological inhibitors. The final concentration of DMSO in the medium never exceeded 0.2% (v/v), and the control group received the equivalent concentration of solvent.

## Adeno/lentiviral infection

Adenoviral siRNA that targets Nox4 (Ad.siNox4), MMP9 (Ad.siMMP9) and Ad.siGFP were previously described (Siddesha et al., 2013). CF were infected at ambient temperature with the virus in PBS at the indicated multiplicity of infection (MOI). After 1 h, the medium containing virus was replaced with culture medium supplemented with 0.5% BSA. Assays were carried out after 24 h. The transfection efficiency with adenoviral vectors was near 100% as evidenced by the expression of GFP in CF infected with Ad.GFP. Lentiviral shRNA that targets p65 and c-Jun were previously described (Venkatesan et al., 2013), and used at a

MOI of 0.5 for 48 h. At the indicated MOI, adeno/lentiviral infection had no off-target effects, nor affected CF adherence, shape and viability (trypan blue-dye exclusion; data not shown).

### Determination of hydrogen peroxide generation

Hydrogen peroxide levels were quantified as previously described (Siddesha et al., 2014; Siddesha et al., 2013) using the Amplex® Red Hydrogen Peroxide/Peroxidase Assay Kit. The generated hydrogen peroxide was quantified by measuring the absorbance of the Amplex® Red reagent at 565 nm. A standard curve was generated using known concentrations of hydrogen peroxide (between 0.001 to 0.1 mM).

### Measurement of TBARS

Following Ang II treatment with and with out interventions for 2 h, fibroblast cultures ($2\times10^7$ cell) were scraped into 1 ml ice-cold PBS, sonicated (5 sec, 3X, 40V) over ice, and undiluted homogenates were used to quantify TBARS according to the manufacturer. A standard curve (0–50 μM) was generated using the TBA MDA Standard. $H_2O_2$ (100 μM) served as a positive control. The absorbance was monitored at an excitation wavelength of 530 nm and an emission wavelength of 550 nm. The results are presented as fold change from untreated.

### mRNA expression-RT-qPCR

DNA-free total RNA was prepared using the RNAqueous®-4PCR kit (Ambion). RNA quality was assessed by capillary electrophoresis using the Agilent 2100 Bioanalyzer (Agilent Technologies, Palo Alto, CA). All RNA samples used for quantitative PCR had RNA integrity numbers greater than 9.0 (scale = 1–10) as assigned by default parameters of the Expert 2100 Bioanalyzer software package (v2.02). IL-18 expression was analyzed by RT-qPCR using Taqman probes (Mm00434225_m1). β-actin served as the internal control (Mm01324804_m1). No template controls were also performed for each assay, and samples processed without the reverse transcriptase step served as negative controls. Each cDNA sample was run in triplicate, and the amplification efficiencies of all primer pairs were determined by serial dilutions of input template. Data were analyzed using the 2−ΔΔCt method.

### Immunoblotting and ELISA

CF were solubilized with Nonidet P-40 lysis buffer (0.5% Nonidet P-40, 10 mM Tris-HCl, pH 7.4, 150 mM NaCl, 3 mM *p*-amidinophenylmethanesulfonyl fluoride, 5 mg/ml aprotinin, 2 mM sodium orthovanadate, 5 mM EDTA). Equal amounts of samples were separated by 10% SDS-PAGE, transferred to polyvinylidene difluoride membrane (Hybond-P, GE Healthcare), incubated in blocking buffer (2% nonfat dry milk in Tris-buffered saline) for 1 h at room temperature, and probed overnight at 4°C with primary antibodies diluted in 2% nonfat dry milk in Tris-buffered saline containing 0.05% Tween 20 (TTBS). The blots were rinsed in TTBS for 30 min and then incubated in horseradish peroxidase-conjugated secondary antibodies in 5% milk in TTBS for 1 h and developed using a chemiluminescent substrate (SuperSignal™ West Pico + 5% SuperSignal™ Femto, Pierce). The

immunoreactive bands migrated at expected relative mobilities were quantified using a CCD image sensor (ChemiDocXRS, Bio-Rad) and software (Quantity One, Bio-Rad). Precision Plus Protein™ dual color standards (range 10–250 kDa; Bio-Rad) were run each time. The membranes were generally probed not more than twice, including the internal control following stripping in between using Restore™ Western blot Stripping Buffer. However, when the molecular weights of the target proteins varied widely, the membrane was used 3 times. Secreted IL-18 levels in culture supernatants were analyzed by ELISA according to manufacturer's instructions.

### Lysyl oxidase activity

The quiescent fibroblasts were exposed to Ang-II (10-7M) for 24 h in 0,5% BSA-RPMI 1640 medium. The conditioned medium was used for LOX activity assay using diaminopentane as a substrate and Amplex red as a $H_2O_2$ probe, and has been described previously (Palamakumbura and Trackman, 2002; Voloshenyuk et al., 2011). After 20 min of incubation at 22°C, $H_2O_2$ production in media was assessed with and without 0.5 M β-aminopropionitrile (BAPN), an irreversible LOX inhibitor. Pilot experiments indicated that this incubation time corresponds to the linear portion of the enzymatic activity curve. LOX activity was calculated as the $H_2O_2$ production that was inhibited by BAPN. Measurements were made on a fluorescent spectrophotometer (Spectra Max, Molecular Devices) at excitation and emission wavelengths of 563 and 587 nm, respectively. All results were normalized to total cell protein and expressed as fold change from untreated controls.

### AT1/Nox4 binding interaction *in vitro*-GST pull-down assay

The interaction *in vitro* between mouse Nox4 and the terminal cytoplasmic domain of mouse angiotensin receptor type 1 was investigated using a GST pull-down assay, essentially as described previously for the interaction between rat AT1 and Nox1 (Valente et al., 2012). DNA encoding C-terminal amino acids 303 to 359 of AT1 was amplified from full length mouse AT1 cDNA (MC201798, Origene, Rockville, MD) using the PCR primers 5′-gaattCCGGCTTTCTGGGGAAAAAATTTAAAAAGTATTTCCTC-3′, and 5′-TCACTCCACCTCAGAACAAGACGC-3′, and cloned into pCR2.1-TOPO (Invitrogen). The insert was excised with *Eco*RI and ligated into the *Eco*RI site of pGEX-3X (GE Health Care) to encode a GST-$AT1_{(303\text{-}359)}$ fusion protein. Mouse Nox4 cDNA was a kind gift from Botond Banfi (University of Iowa-Carver Collage of Medicine, Iowa City, IA). GST and GST-$ATI_{(303\text{-}359)}$ were induced in the Rosetta™ strain of E.coli (EMD Chemical Inc) with 1mM IPTG and bacterial cell lysates prepared using standard procedures.

Binding interactions were carried out between GST and GST-$ATI_{(303\text{-}359)}$ fusion protein immobilized on GSH-Sepharose (GE Health Care), and *in vitro* synthesized [$^{35}$S]-labeled mouse Nox4. Volumes of fusion protein lysates, previously determined to give equal loading of the GSH-Sepharose, were mixed for 30 min at room temperature with 50 μl of a 50% suspension of washed GSH-Sepharose in PBS (145 mM NaCl, 10 mM $Na_2HPO_4$, pH 7.3). The suspensions were washed ×3 with PBS and ×3 with PBS containing 0.05% Triton X-100, and resuspended to 476 μl in PBS/0.05%. Nox4 was synthesized and labeled *in vitro* with L-[$^{35}$S]-methionine (PerkinElmer NEG709A, 1175Ci/mmol) using the TNT® Coupled

Reticulocyte Lysate System (Promega) and T7 RNA polymerase. The pull down binding assay was carried out exactly as described previously (Valente et al., 2012).

## Cell proliferation

CF were seeded in triplicate at a concentration of $1\times10^3$ cells/well in 200 μL of complete medium (RPMI 1640/5 mM glucose/10% heat-inactivated FBS/antibiotics, pH 7.3) in 96-well flat-bottom plates (Costar, Corning, NY, USA). After 24 h incubation, the medium was replaced with conditioning medium (RPMI 1640/5 mM glucose/0.5% BSA/antibiotics, pH 7.3), and then incubated for an additional 48 h. The cells were treated with Ang-II for 48 h and pulsed with 0.5 μCi/well [$^3$H]Thymidine (TdR) for the last 16 h of the incubation period. Cells were then harvested on to membranes and the incorporated [$^3$H]TdR was measured using a liquid-scintillation counter (Beckman LS6500). Results were expressed as fold increases above unstimulated controls.

CF proliferation was also analyzed by CyQUANT® assay (Invitrogen, Carlsbad, CA) as previously described (Colston et al., 2007). Briefly, second-passage CFs were plated into 96-well plates at 3,000 cells per well and allowed to attach overnight. After 24 h, the cells were fed with serum-free medium containing 0.5% BSA and incubated for an additional 24 h. Cells were then continuously stimulated with Ang-II in serum-free medium for 48 h before analysis

## Cell migration

CF migration was quantified as described previously (Siddesha et al., 2014; Siddesha et al., 2013; Somanna et al., 2015) using BioCoat™ Matrigel™ invasion chambers and 8.0-μm pore polyethylene terephthalate membranes with a thin layer of Matrigel™ basement membrane matrix. Cultured CF were trypsinized and suspended in RPMI + 0.5% bovine serum albumin, and 1 ml containing $2.0 \times 10^5$ cells/ml was layered on the coated insert filters. Cells were stimulated with Ang-II ($10^{-7}$M). The lower chamber contained medium containing 10% serum. Plates were incubated at 37 °C for 12 h. Membranes were washed with phosphate-buffered saline, and non-invading cells on the upper surface were removed using cotton swabs. Cells migrating to the lower surface of the membrane were determined at $A_{540\ nm}$ using a commercially available MTT assay kit.

## Sircol™ Collagen assay

The effect of Ang-II on collagen expression in CF was determined by Sircol™ Collagen assay (Biocolor, Newtownabbey, N. Ireland) as previously described (Colston et al., 2007; Somanna et al., 2015). The assay is based on the specific binding of the anionic dye Sirus red to the basic amino acid residues of collagen. Briefly, second-passage CFs were plated into 100-mm culture dishes at 80% confluency, allowed to attach overnight, and the medium changed the following day to a serum-free medium containing 0.5% BSA. After 24 h, CFs were stimulated with Ang-II ($10^{-7}$M) in serum-free medium for 72 h. Levels of soluble collagens released into culture media by CF incubated with Ang-II or saline vehicle were determined by spectrophotometry according to the manufacturer's instructions. Each collagen assay included standard curves using purified soluble collagen supplied by the manufacturer.

### Statistical analysis

All data are expressed as mean ± SE. Statistical significance was determined by one-way analysis of variance followed by Tukey's post-hoc test. Differences are considered significant if the *P* value is less than or equal to 0.05. Though a representative immunoblot is shown in the main figures, changes in protein/phosphorylation levels from three independent experiments were semi-quantified by densitometry, and were shown as ratios and fold changes from untreated or respective controls at the bottom of the panels whenever the results are less clear.

## Results

### Nox4 and ROS mediate Ang-II-induced cardiac fibroblast proliferation and migration

Ang-II is a potent inducer of oxidative stress. Murine CF predominantly express Nox4 (Colston et al., 2005). Therefore, we investigated whether Ang-II-induced CF proliferation and migration are Nox4 dependent. As shown in Fig. 1A, Ang-II induced CF proliferation, and this effect was markedly attenuated by the AT1 receptor antagonist losartan. These results were confirmed by the CyQUANT® assay (data not shown). Further, knockdown of Nox4 or pretreatment with the Nox inhibitor DPI each attenuated CF proliferation (Fig. 1A). Similarly, Ang-II induced CF migration, and Nox4 knockdown and DPI each attenuated this effect (Fig. 1B). Further, knockdown of Nox4 and DPI pre-treatment each attenuate Ang-II-induced $H_2O_2$ production (Fig. 1C) and lipid peroxidation as evidenced by reduced levels of TBARS (Fig. 1C, right hand). Our results also demonstrate that the reduction in Ang-II-induced CF proliferation and migration were not due to cell death, since only low levels of mono and oligonucleosomal fragmented DNA were detected in the cytoplasmic extracts (Fig. 1D). Moreover, activated caspase-3 levels remained unchanged (Fig. 1D, inset). Of note, DMSO and Ad.siGFP used as controls had no basal effects on all of the parameters studied (data not shown). These results indicate that Ang-II induces CF proliferation and migration in part via Nox4 and ROS (Fig. 1).

To confirm the role of oxidative stress in Ang-II-induced CF proliferation and migration, we treated CF with the antioxidant NAC, and the cell permeable SOD mimetics Tempol, MnTBAP and MnTMPyP prior to Ang-II addtion. The results show that similar to DPI, NAC (data not shown) and all three SOD mimetics attenuated CF proliferation (Fig. 2A), migration (Fig. 2B), and $H_2O_2$ and TBARS generation (Fig. 2C). However, they failed to modulate cell viability, indicating that all three SOD mimetics exerts anti-proliferative and migratory effects by attenuating oxidative stress (Fig. 2).

### Nox4 and ROS mediate Ang-II-induced IL-18 expression and MMP9 activation

IL-18 is a proinflammatory cytokine that exerts both mitogenic and migratory effects (Fix et al., 2011; Siddesha et al., 2014; Valente et al., 2013). MMP9 activation contributes to extracellular matrix degradation and cell migration. Therefore, we next examined whether Ang-II induces IL-18 expression and MMP9 activation in CF via Nox4 and ROS. Indeed, Ang-II significantly increased IL-18 mRNA expression in CF, and both Nox4 knockdown and DPI each attenuated its expression (Fig. 3A). Further, Nox4 knockdown and DPI each attenuated Ang-II-induced IL-18 and IL-18Rα protein levels (Fig. 3B) and IL-18 secretion

(Fig. 3C). Similarly, Nox4 knockdown and DPI each attenuated Ang-II-induced MMP9 activation (Fig. 3D) and activity (Fig. 3E). Knockdown of Nox4 and DPI pretreatment also attenuated Ang-II-induced collagen expression (Fig. 3F) and secretion (Fig. 3G). Of note, DMSO and Ad.siGFP used as controls had no basal effects on all of the parameters studied (data not shown). Together, these results indicate that Nox4 and ROS contribute critically to Ang-II-induced IL-18 expression, MMP9 activation and collagen expression and secretion CF (Fig. 3).

### Nox4 and ROS mediate Ang-II-induced NF-κB and AP-1 activation

Activation of the redox-senstive nuclear transcription factors NF-κB and AP-1 is known to regulate both IL-18 and MMP9 (Chandrasekar et al., 2006; Tone et al., 1997). Here we show that Nox4 knockdown and DPI pretreatment each attenuated Ang-II-induced NF-κB/p65 (Fig, 4A, upper and lower panels) and AP-1/c-Jun activation (Fig, 4B, upper and lower panels), as seen by a reduction in their phosphorylated levels. Further, knockdown of p65 and c-Jun each attenuated mature IL-18 protein levels (Fig. 4C, upper panel) and MMP9 activation (Fig. 4C, lower panel). Together, these results indicate Ang-II-induced IL-18 expression and MMP9 activation are redox sensitive, and are dependent on Nox4 and ROS mediated NF-κB and AP-1 activation in CF (Fig. 4).

### IL-18 and MMP9 mediate Ang-II-induced CF proliferation and migration

We have demonstrated that Nox4 and ROS mediate Ang-II-induced IL-18 expression and MMP9 activation (Fig. 3). Since IL-18 exerts potent pro-mitogenic effects (Fix et al., 2011; Siddesha et al., 2014; Valente et al., 2013), we investigated whether IL-18 mediates Ang-II-induced CF proliferation and migration. The results in Fig. 5A show that pre-incubation with IL-18 neutralizing antibodies or IL-18BP-Fc chimera each markedly suppressed Ang-II-induced CF proliferation. Further, both attenuated Ang-II-induced collagen Iα1 and IIIα1 expression (Fig. 5B). Further, blocking IL-18 signaling inhibited Ang-II-induced CF migration (Fig. 5C), as was MMP9 knockdown (Fig. 5C). Together these results indicate that IL-18 and MMP9 mediate Ang-II's pro-mitogenic and pro-migratory effects on CF (Fig. 5).

### Nox4 physically associates with AT1, and Ang-II but not IL-18 increases their binding

We have previously reported that AT1 physically associates with Nox2 in primary cardiomyocytes and that Ang-II enhances their interaction *in vivo* (Shanmugam et al., 2011). Therefore, we investigated whether AT1 also binds Nox4. Using GST pull-down assays, we found that labeled Nox4 bound to a GST fusion protein containing the C-terminal region (amino acids 303–359) of AT1 but not to GST itself (Fig. 6A). To determine if Nox4 interacts with AT1 *in vivo*, we carried out reciprocal immunoprecipitation and immunoblotting (co-IP/IB) of solubilized membrane preparations and whole cell lysates from CF treated or not with Ang-II for 15 min. Our results indicate that while AT1 and Nox4 do associate *in vivo* at low levels, this association was increased with Ang-II treatment (Fig. 6B, left). Similar results were obtained when the converse IP/IB experiments were carried out (Fig. 6B, right). Since IL-18 mediates part of the Ang-II effects (Fig. 5), we next examined whether IL-18 regulates AT1 binding to Nox4. Unlike Ang-II, IL-18 appears not to modulate the basal binding of AT1/Nox4 (Fig. 6C), indicating that although IL-18 mediates part of Ang-II signaling, it fails to modulate AT1/Nox4 interaction. Together, these

results indicate that Nox4 physically associations with AT1, and Ang-II, but not IL-18, enhances their binding in CF (Fig. 6).

### The Nox1/Nox4 inhibitor GKT137831 inhibits Ang-II-induced CF proliferation and migration

Nox4 plays a critical role in Ang-II-induced CF proliferation and migration (Fig. 1). GKT137831 (GKT) is a small molecule Nox1/Nox4-specific dual inhibitor (Laleu et al., 2010). Its effects on CF proliferation and migration have yet to be investigated. Our results show for the first time that GKT markedly inhibited Ang-II-induced $H_2O_2$ production in CF (Fig. 7A). More importantly, GKT attenuated AT1/Nox4 interaction (Fig. 7B). Further, GKT inhibited IL-18, IL-18Rα, and CTGF expression (Fig. 7C) and MMP9 activation (Fig. 7D) in CF. GKT also inhibited collagens Iα1 and IIIα1 expression and secretion (Fig. 7E), and activation of the collagen crosslinking enzyme LOX (Fig. 7F). Notably, GKT also attenuated Ang-II-induced CF proliferation (Fig. 8A) and migration (Fig. 8B). However, GKT did not affect CF viability (Fig. 8C). Together, these results demonstrate that GKT suppresses CF proliferation, migration, and expression of various proinflammatory and pro-fibrotic markers in CF, and suggest that GKT may have a therapeutic potential in hypertensive heart disease (Fig. 7 and Fig. 8).

## Discussion

Fibroblasts are the majority cell type in the normal heart, and contribute significantly to cardiac structure and function. By regulating extracellular matrix deposition and degradation, CF play a critical role in ECM homeostasis (Chen and Frangogiannis, 2010; Kong et al., 2014). CF also express multiple cytokines, chemokines and growth factors under physiological conditions that not only affect CF function in an autocrine manner, but also regulate cardiomyocyte function and survival in a paracrine manner. However, following injury or under chronic stress conditions such as hypertension, CF migrate, differentiate into myofibroblasts, proliferate, and actively deposit large amounts of ECM, resulting in reactive or reparative fibrosis and contractile depression. Here we have demonstrated that Ang-II stimulated both migration and proliferation of fibroblasts via AT1/Nox4-dependent $H_2O_2$ production, IL-18 and IL-18Rα induction, collagens I and III expression, collagens secretion, and MMP9 activation. Further, Ang-II increased AT1/Nox4 physical association (Fig. 7), and pre-treatment with GKT137831, a small molecule Nox1/Nox4 dual inhibitor, or knockdown of Nox4 attenuated Ang-II's pro-mitogenic and pro-migratory effects. Notably, GKT137831 attenuated AT1/Nox4 interaction. Targeting IL-18, Nox4 or AT1/Nox4 interaction may have a therapeutic potential in HHD.

Cardiac fibrosis is a characteristic feature of HHD in humans and in experimental animals infused chronically with Ang-II, and both AT1 blockers and angiotensin-converting enzyme inhibitors exert anti-fibrotic effects and attenuate adverse cardiac remodeling. Here we show that the AT1 blocker losartan attenuates Ang-II-induced CF migration and proliferation by blocking the induction of the pro-inflammatory cytokine IL-18 and activation of the matrix-degrading metalloproteinase MMP9. These effects appear to be attributed to inhibition of oxidative stress. In fact, pre-treatment with the Nox inhibitor DPI inhibited Ang-II-induced IL-18/IL-18Rα expression, collagen expression and secretion, and MMP9 activation. DPI

also attenuated Ang-II-induced CF proliferation and migration. These results suggest a critical role for oxidative stress in the pro-mitogenic and pro-migratory effects of Ang-II in CF.

In this study, a 30-min pretreatment with 10 μM DPI markedly attenuated Ang-II-induced $H_2O_2$ production and TBARS generation in the CF. Pretreatment with DPI also attenuated Ang-II-induced fibroblast proliferation and migration by attenuating multiple redox-senstive mitogenic and migratory factors. However, DPI is a flavoprotein inhibitor, and has been shown to target multiple sources of oxidative stress, including cytochrome P450 mono-oxygenases, NO synthase, and mitochondria-derived ROS (Aldieri et al., 2008). Further, in some studies, a 3-hour pretreatment with DPI has been shown to induce oxidative stress, rather than inhibiting it (Riganti et al., 2004). Similar non-specific effects were also reported with apocyanin (Heumuller et al., 2008), another widely used Nox inhibitor, suggesting that results obtained with DPI and apocyanin need to be interpreted with caution, and should be accompanied by another method that specifically targets the Nox isoform being studied. In this study, therefore, we also targeted Nox4 with adenoviral siRNA. Transduction with Ad.siNox4 specifically and significantly reduced Nox4 in cardiac fibroblasts, and silencing Nox4 attenuated Ang-II-induced oxidative stress and its downstream targets. These inhibitory effects on $H_2O_2$ production were mimicked by the antioxidant NAC and the SOD mimetics Tempol, MnTBAP and MnTMPyP. TBAR levels, and fibroblast proliferation and migration were also inhibited, indicating that Ang-II-induced CF migration and proliferation are oxidative stress-responsive.

The NADPH oxidases (Noxs) play a critical role in ROS generation under physiological conditions, and regulate the redox status and various redox-sensitive signal transduction pathways in a cell. Their increased activation and/or expression contribute to cardiovascular diseases, including cardiac fibrosis during chronic hypertension. Colston et al. reported that CF express Nox4 predominantly (Colston et al., 2005). Though primarily expressed in lymphoid tissue, Nox5 is also expressed in human CF (Bedard et al., 2012; Cucoranu et al., 2005). However, regulation of Nox4 and Nox5 are reported to be very different in these cells. For example, in TGF-β-induced human fibroblast differentiation into myofibroblasts, expression of Nox4 is increased by at least 16 fold, while that of Nox5 is markedly suppressed (Cucoranu et al., 2005). In mouse however, a functional Nox5 gene is absent, and the dominant form of oxidase expressed in CF is Nox4 (Colston et al., 2005). Here we show that knockdown of Nox4 markedly attenuates Ang-II-induced $H_2O_2$ production, IL-18 and collagen expression, MMP9 and LOX activation, and importantly CF migration and proliferation. These results indicate that Nox4 promotes all three critical phases of fibroblast biology under conditions of stress - differentiation, migration, and proliferation - that ultimately results in cardiac fibrosis.

The 5′-flanking regions of *IL18*, *COL1A1*, and *COL3A1* genes contain binding sites for multiple redox-sensitive response elements, including AP-1, NF-κB or Sp-1. In fact, the promoter region of *IL18* contains both NF-κB and AP-1 responsive elements (Tone et al., 1997), and $H_2O_2$ induces its expression in a NF-κB-dependent manner (Chandrasekar et al., 2003). In addition to IL-18, $H_2O_2$ also upregulates IL-18Rα expression (Chandrasekar et al., 2003), suggesting an amplification of the IL-18 stimulus-response pathway in the induction/

perpetuation of inflammation. IL-18 is also a potent inducer of collagen gene expression, and both collagens I and III are also regulated by Sp1, AP-1 or NF-κB. Of note, NF-κB is also an essential regulator of Nox4 (Lu et al., 2010). We have also demonstrated that neutralizing IL-18 or silencing MMP9 attenuates Ang-II-induced CF migration. We have previously reported that IL-18 can induce MMP9 expression via activation of NF-κB and AP-1 (Chandrasekar et al., 2006). This suggests that while Ang-II can induce both IL-18 and MMP9 independently through activation of NF-κB and AP-1 in CF, upon induction, IL-18 can also amplify Ang-II signaling by upregulating MMP9. Therefore, the relationship between IL-18 and MMP9 appears to be both direct and indirect: Ang-II→MMP9, Ang-II→IL-18, and IL-18→MMP9. Therefore, neutralizing IL-18 may blunt amplification in Ang-II inflammatory signaling and may exert protective effects in HHD.

Our results also show that GKT137831 (GKT) inhibited Ang-II-induced $H_2O_2$ production, expression and activation of inflammatory cytokines, pro-fibrotic markers, CF proliferation and migration *in vitro*. GKT also downregulated the expression of the collagen cross-linking enzyme LOX. Since *LOX* is a NF-κB and AP-1 responsive gene (Papachroni et al., 2010), it is possible that GKT may inhibit Ang-II-induced LOX and other markers of inflammation and remodeling by targeting the oxidative stress-responsive NF-κB and AP-1 activation in cardiac fibroblasts. GKT is a small molecule Nox1/4-specific dual inhibitor that has weak inhibitory activity towards Nox2 (Laleu et al., 2010). However, it exerts neither antioxidant nor ROS scavenging effects. Recently its therapeutic potential has been reported *in vivo*. In a transgenic mouse model with Nox4 overexpression specifically in cardiomyocytes, treatment with GKT attenuated Ang-II-induced increases in oxidative stress, activation of Akt-mTOR and NF-κB signaling, and cardiac fibrosis (Zhao et al., 2015). It is possible that this reduction in fibrosis after GKT treatment may be a consequence of attenuated pro-fibrotic gene expression and fibroblast proliferation and migration, as well as collagen deposition, as we have demonstrated here *in vitro*. Increased Nox4 activation has also been shown to play a critical role in hepatic fibrosis, and GKT, when used as a preventive or therapeutic strategy, markedly reduced fibrosis (Jiang et al., 2012). In those studies, GKT was also shown to exert anti-apoptotic effects. This dual inhibitor also attenuates hypoxia-induced pulmonary vascular cell proliferation (Green et al., 2012). Thus, GKT, which exhibits good bioavailability and tolerability upon oral administration in both experimental models and humans, may have a therapeutic potential in cardiac fibrosis and adverse remodeling in HHD. Importantly, our data show that GKT also attenuates AT1/Nox4 physical interaction. At present we are not sure whether this AT1/Nox4 binding interaction is an integral step in an Ang-II-induced Nox4 activation pathway. Of note, AT1 lacks intrinsic kinase activity, therefore the binding of AT1/Nox4 may provide a better substrate for the phosphorylation and activation of Nox4 by the relevant cellular kinase. For example, Src kinase can induce Nox4 phosphorylation (Xi et al., 2013), and Ang-II is known to activate Src in cardiac fibroblasts via AT1 (Godeny and Sayeski, 2006). We are currently investigating whether the AT1/Nox4 binding interaction is required for full Nox4 modification by Src or some other kinase.

Previously we reported that Ang-II enhances AT1/Nox1 binding and stimulates arterial smooth muscle cell proliferation and migration through AT1, Nox1, and IL-18 (Valente et al., 2012). We have also reported that AT1 binds Nox2 and mediates Ang-II-induced

cardiomyocyte hypertrophy in part via Nox2/TCF/LEF- and CREB-dependent WISP1 induction (Shanmugam et al., 2011). These data indicate that AT1 can physically associate with Nox1, 2 or 4 in a cell type-specific manner and suggest the possibility of related AT1 binding motifs in these Nox isoforms. Studies are in progress to identify these motifs with a goal of generating small molecule/peptide inhibitors that will block AT1/Nox interaction. Such novel inhibitors, besides GKT, may have therapeutic potential in HHD. Of note, activation of Nox4 is not always detrimental. In fact, its activation has been shown to exert beneficial effects, but in a cell- and context-dependent manner (Schroder et al., 2012; Shah, 2015). However, excessive generation of ROS for prolonged periods of time inevitably leads to cardiac pathology.

Together, our studies demonstrate that Ang-II induces cardiac fibroblast proliferation and migration in part via Nox4/ROS-dependent IL-18 induction and MMP9 activation, and may involve AT1/Nox4 binding. Blocking AT1 and Nox4 physical association may be an alternative and attractive strategy to blunt Ang-II-induced adverse cardiac remodeling in HHD. Our results also suggest that the Nox1/Nox4-specific inhibitor GKT137831 has a therapeutic potential in HHD.

## Acknowledgments

BC is a recipient of the Department of Veterans Affairs *Research Career Scientist* award, and is supported by the U.S. Department of Veterans Affairs, Office of Research and Development-Biomedical Laboratory Research and Development (ORD-BLRD) Service Award VA-I01-BX002255. PD is supported by National Institutes of Health Grants R01HL070241 and R01HL080682. The contents of this report do not represent the views of the Department of Veterans Affairs or the United States government.

## Literature cited

Aldieri E, Riganti C, Polimeni M, Gazzano E, Lussiana C, Campia I, Ghigo D. Classical inhibitors of NOX NAD(P)H oxidases are not specific. Curr Drug Metab. 2008; 9(8):686–696. [PubMed: 18855607]

Bedard K, Jaquet V, Krause KH. NOX5: from basic biology to signaling and disease. Free Radic Biol Med. 2012; 52(4):725–734. [PubMed: 22182486]

Chandrasekar B, Colston JT, de la Rosa SD, Rao PP, Freeman GL. TNF-alpha and H2O2 induce IL-18 and IL-18R beta expression in cardiomyocytes via NF-kappa B activation. Biochem Biophys Res Commun. 2003; 303(4):1152–1158. [PubMed: 12684057]

Chandrasekar B, Mummidi S, Mahimainathan L, Patel DN, Bailey SR, Imam SZ, Greene WC, Valente AJ. Interleukin-18-induced human coronary artery smooth muscle cell migration is dependent on NF-kappaB- and AP-1-mediated matrix metalloproteinase-9 expression and is inhibited by atorvastatin. J Biol Chem. 2006; 281(22):15099–15109. [PubMed: 16554298]

Chen W, Frangogiannis NG. The role of inflammatory and fibrogenic pathways in heart failure associated with aging. Heart Fail Rev. 2010; 15(5):415–422. [PubMed: 20213186]

Colston JT, de la Rosa SD, Koehler M, Gonzales K, Mestril R, Freeman GL, Bailey SR, Chandrasekar B. Wnt-induced secreted protein-1 is a prohypertrophic and profibrotic growth factor. Am J Physiol Heart Circ Physiol. 2007; 293(3):H1839–1846. [PubMed: 17616748]

Colston JT, de la Rosa SD, Strader JR, Anderson MA, Freeman GL. H2O2 activates Nox4 through PLA2-dependent arachidonic acid production in adult cardiac fibroblasts. FEBS Lett. 2005; 579(11):2533–2540. [PubMed: 15848200]

Cucoranu I, Clempus R, Dikalova A, Phelan PJ, Ariyan S, Dikalov S, Sorescu D. NAD(P)H oxidase 4 mediates transforming growth factor-beta1-induced differentiation of cardiac fibroblasts into myofibroblasts. Circ Res. 2005; 97(9):900–907. [PubMed: 16179589]

Fix C, Bingham K, Carver W. Effects of interleukin-18 on cardiac fibroblast function and gene expression. Cytokine. 2011; 53(1):19–28. [PubMed: 21050772]

Godeny MD, Sayeski PP. ANG II-induced cell proliferation is dually mediated by c-Src/Yes/Fyn-regulated ERK1/2 activation in the cytoplasm and PKCzeta-controlled ERK1/2 activity within the nucleus. Am J Physiol Cell Physiol. 2006; 291(6):C1297–1307. [PubMed: 16723512]

Gonzalez A, Lopez B, Diez J. Fibrosis in hypertensive heart disease: role of the renin-angiotensin-aldosterone system. Med Clin North Am. 2004; 88(1):83–97. [PubMed: 14871052]

Green DE, Murphy TC, Kang BY, Kleinhenz JM, Szyndralewiez C, Page P, Sutliff RL, Hart CM. The Nox4 inhibitor GKT137831 attenuates hypoxia-induced pulmonary vascular cell proliferation. Am J Respir Cell Mol Biol. 2012; 47(5):718–726. [PubMed: 22904198]

Heumuller S, Wind S, Barbosa-Sicard E, Schmidt HH, Busse R, Schroder K, Brandes RP. Apocynin is not an inhibitor of vascular NADPH oxidases but an antioxidant. Hypertension. 2008; 51(2):211–217. [PubMed: 18086956]

Iwata M, Cowling RT, Yeo SJ, Greenberg B. Targeting the ACE2-Ang-(1–7) pathway in cardiac fibroblasts to treat cardiac remodeling and heart failure. J Mol Cell Cardiol. 2011; 51(4):542–547. [PubMed: 21147120]

Jiang JX, Chen X, Serizawa N, Szyndralewiez C, Page P, Schroder K, Brandes RP, Devaraj S, Torok NJ. Liver fibrosis and hepatocyte apoptosis are attenuated by GKT137831, a novel NOX4/NOX1 inhibitor in vivo. Free Radic Biol Med. 2012; 53(2):289–296. [PubMed: 22618020]

Kong P, Christia P, Frangogiannis NG. The pathogenesis of cardiac fibrosis. Cell Mol Life Sci. 2014; 71(4):549–574. [PubMed: 23649149]

Laleu B, Gaggini F, Orchard M, Fioraso-Cartier L, Cagnon L, Houngninou-Molango S, Gradia A, Duboux G, Merlot C, Heitz F, Szyndralewiez C, Page P. First in class, potent, and orally bioavailable NADPH oxidase isoform 4 (Nox4) inhibitors for the treatment of idiopathic pulmonary fibrosis. J Med Chem. 2010; 53(21):7715–7730. [PubMed: 20942471]

Lu X, Murphy TC, Nanes MS, Hart CM. PPAR{gamma} regulates hypoxia-induced Nox4 expression in human pulmonary artery smooth muscle cells through NF-{kappa}B. Am J Physiol Lung Cell Mol Physiol. 2010; 299(4):L559–566. [PubMed: 20622120]

McMaster WG, Kirabo A, Madhur MS, Harrison DG. Inflammation, immunity, and hypertensive end-organ damage. Circ Res. 2015; 116(6):1022–1033. [PubMed: 25767287]

Palamakumbura AH, Trackman PC. A fluorometric assay for detection of lysyl oxidase enzyme activity in biological samples. Anal Biochem. 2002; 300(2):245–251. [PubMed: 11779117]

Papachroni KK, Piperi C, Levidou G, Korkolopoulou P, Pawelczyk L, Diamanti-Kandarakis E, Papavassiliou AG. Lysyl oxidase interacts with AGE signalling to modulate collagen synthesis in polycystic ovarian tissue. J Cell Mol Med. 2010; 14(10):2460–2469. [PubMed: 19583806]

Riganti C, Gazzano E, Polimeni M, Costamagna C, Bosia A, Ghigo D. Diphenyleneiodonium inhibits the cell redox metabolism and induces oxidative stress. J Biol Chem. 2004; 279(46):47726–47731. [PubMed: 15358777]

Schroder K, Zhang M, Benkhoff S, Mieth A, Pliquett R, Kosowski J, Kruse C, Luedike P, Michaelis UR, Weissmann N, Dimmeler S, Shah AM, Brandes RP. Nox4 is a protective reactive oxygen species generating vascular NADPH oxidase. Circ Res. 2012; 110(9):1217–1225. [PubMed: 22456182]

Shah AM. Parsing the role of NADPH oxidase enzymes and reactive oxygen species in heart failure. Circulation. 2015; 131(7):602–604. [PubMed: 25589558]

Shanmugam P, Valente AJ, Prabhu SD, Venkatesan B, Yoshida T, Delafontaine P, Chandrasekar B. Angiotensin-II type 1 receptor and NOX2 mediate TCF/LEF and CREB dependent WISP1 induction and cardiomyocyte hypertrophy. J Mol Cell Cardiol. 2011; 50(6):928–938. [PubMed: 21376054]

Siddesha JM, Valente AJ, Sakamuri SS, Gardner JD, Delafontaine P, Noda M, Chandrasekar B. Acetylsalicylic acid inhibits IL-18-induced cardiac fibroblast migration through the induction of RECK. J Cell Physiol. 2014; 229(7):845–855. [PubMed: 24265116]

Siddesha JM, Valente AJ, Sakamuri SS, Yoshida T, Gardner JD, Somanna N, Takahashi C, Noda M, Chandrasekar B. Angiotensin II stimulates cardiac fibroblast migration via the differential regulation of matrixins and RECK. J Mol Cell Cardiol. 2013; 65:9–18. [PubMed: 24095877]

Somanna NK, Yariswamy M, Garagliano JM, Siebenlist U, Mummidi S, Valente AJ, Chandrasekar B. Aldosterone-induced cardiomyocyte growth, and fibroblast migration and proliferation are mediated by TRAF3IP2. Cell Signal. 2015; 27(10):1928–1938. [PubMed: 26148936]

Takac I, Schroder K, Zhang L, Lardy B, Anilkumar N, Lambeth JD, Shah AM, Morel F, Brandes RP. The E-loop is involved in hydrogen peroxide formation by the NADPH oxidase Nox4. J Biol Chem. 2011; 286(15):13304–13313. [PubMed: 21343298]

Toldo S, Mezzaroma E, O'Brien L, Marchetti C, Seropian IM, Voelkel NF, Van Tassell BW, Dinarello CA, Abbate A. Interleukin-18 mediates interleukin-1-induced cardiac dysfunction. Am J Physiol Heart Circ Physiol. 2014; 306(7):H1025–1031. [PubMed: 24531812]

Tone M, Thompson SA, Tone Y, Fairchild PJ, Waldmann H. Regulation of IL-18 (IFN-gamma-inducing factor) gene expression. J Immunol. 1997; 159(12):6156–6163. [PubMed: 9550417]

Tsutsumi Y, Matsubara H, Ohkubo N, Mori Y, Nozawa Y, Murasawa S, Kijima K, Maruyama K, Masaki H, Moriguchi Y, Shibasaki Y, Kamihata H, Inada M, Iwasaka T. Angiotensin II type 2 receptor is upregulated in human heart with interstitial fibrosis, and cardiac fibroblasts are the major cell type for its expression. Circ Res. 1998; 83(10):1035–1046. [PubMed: 9815151]

Valente AJ, Yoshida T, Izadpanah R, Delafontaine P, Siebenlist U, Chandrasekar B. Interleukin-18 enhances IL-18R/Nox1 binding, and mediates TRAF3IP2-dependent smooth muscle cell migration. Inhibition by simvastatin. Cell Signal. 2013; 25(6):1447–1456. [PubMed: 23541442]

Valente AJ, Yoshida T, Murthy SN, Sakamuri SS, Katsuyama M, Clark RA, Delafontaine P, Chandrasekar B. Angiotensin II enhances AT1-Nox1 binding and stimulates arterial smooth muscle cell migration and proliferation through AT1, Nox1, and interleukin-18. Am J Physiol Heart Circ Physiol. 2012; 303(3):H282–296. [PubMed: 22636674]

Venkatesan B, Valente AJ, Das NA, Carpenter AJ, Yoshida T, Delafontaine JL, Siebenlist U, Chandrasekar B. CIKS (Act1 or TRAF3IP2) mediates high glucose-induced endothelial dysfunction. Cell Signal. 2013; 25(1):359–371. [PubMed: 23085260]

Voloshenyuk TG, Landesman ES, Khoutorova E, Hart AD, Gardner JD. Induction of cardiac fibroblast lysyl oxidase by TGF-beta1 requires PI3K/Akt, Smad3, and MAPK signaling. Cytokine. 2011; 55(1):90–97. [PubMed: 21498085]

Xi G, Shen XC, Wai C, Clemmons DR. Recruitment of Nox4 to a plasma membrane scaffold is required for localized reactive oxygen species generation and sustained Src activation in response to insulin-like growth factor-I. J Biol Chem. 2013; 288(22):15641–15653. [PubMed: 23612968]

Yu Q, Vazquez R, Khojeini EV, Patel C, Venkataramani R, Larson DF. IL-18 induction of osteopontin mediates cardiac fibrosis and diastolic dysfunction in mice. Am J Physiol Heart Circ Physiol. 2009; 297(1):H76–85. [PubMed: 19429811]

Zhao QD, Viswanadhapalli S, Williams P, Shi Q, Tan C, Yi X, Bhandari B, Abboud HE. NADPH oxidase 4 induces cardiac fibrosis and hypertrophy through activating Akt/mTOR and NFkappaB signaling pathways. Circulation. 2015; 131(7):643–655. [PubMed: 25589557]

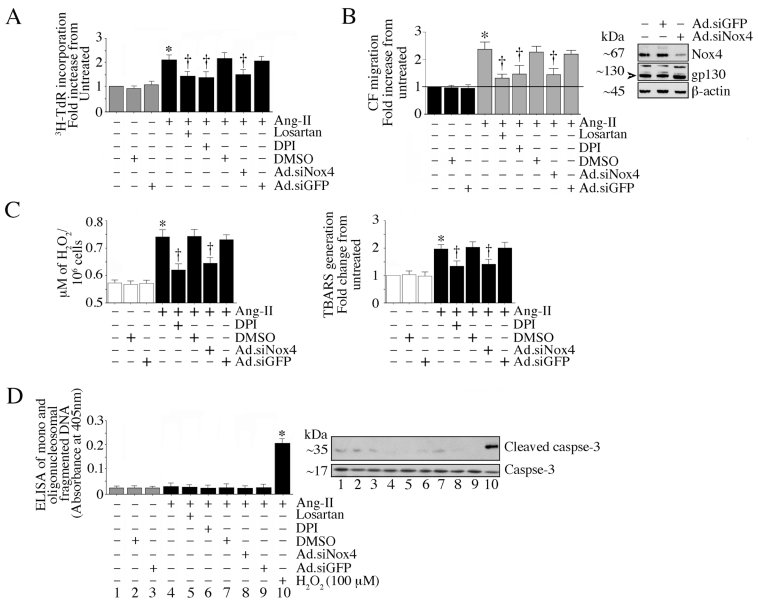


**Fig. 1. Angiotensin (Ang)-II stimulates adult mouse cardiac fibroblast (CF) proliferation and migration via AT1, Nox4, and ROS**

A, Ang-II stimulates CF proliferation via AT1, Nox4 and ROS. Second passage CF at 70–80% confluence were made quiescent by incubating in medium supplemented with 0.5% BSA for 48 h. The quiescent CF were then treated with the AT1 antagonist losartan potassium (10 μM for 1 h) or the NADPH oxidase and flavoprotein inhibitor DPI (10 μM in DMSO for 30 min) prior to Ang-II ($10^{-7}$M) addition. Studies were also performed using CF infected with Ad.siNox4 (MOI 100 for 48 h). DMSO alone (not more than 0.2% v/v in the medium) and Ad.siGFP served as controls. Proliferation assays (incorporation of $^{3}$H-thymidine into DNA) were carried out after 48 h. B, Ang-II stimulates CF migration via AT1, Nox4 and ROS. CF described as in A were layered on Matrigel™ basement membrane matrix-coated filters, and then treated with Ang-II ($10^{-7}$M) for 12 h. The lower chamber contained the medium with 10% serum. Cells migrating to the other side of the membrane were quantified using MTT assay. In separate experiments, CF were layered on Matrigel™ basement membrane matrix-coated filters were incubated with Losartan or DPI prior to Ang-II addition. Studies were also performed by layering CF infected with Ad.siNox4 for 48 h and then treated with Ang-II for 12 h. Knockdown of Nox4 was confirmed by immunoblotting (right hand panel). The IL-6 signal transducer gp130 served as an off target control. β-actin served as a loading control (n=3). C, Nox4 knockdown or DPI pre-treatment inhibit Ang-II-induced hydrogen peroxide ($H_2O_2$) production and lipid peroxidation. The CF infected with Ad.siNox4 (MOI100 for 24 h) or treated with DPI (10 μM in DMSO for 30 min) were incubated with Ang-II ($10^{-7}$M) for 30 min ($H_2O_2$ production) or 2 h (TBARS). $H_2O_2$ levels were quantified using the Amplex® Red Hydrogen Peroxide/Peroxidase Assay Kit. Lipid peroxidation was determined using the TBARS Assay kit. D, Ang-II, DPI treatment or Nox4 knockdown does not induce cell death. CF treated as in A were analyzed for mono and oligonucleosomal fragmented DNA in cytoplasmic extracts using a cell death ELISA. $H_2O_2$ (100 μM for 8h) served as a positive control. Total (~35 kDa) and the cleaved (active) form of caspase-3 (p17/19) at 8 h were analyzed by immunoblotting using cleared

whole cell lysates, and a representative immunoblot from three independent experiments is shown in the inset. A–D, *$P$ < 0.001 vs. untreated, †$P$ < at least 0.05 vs. Ang-II (n = 12).

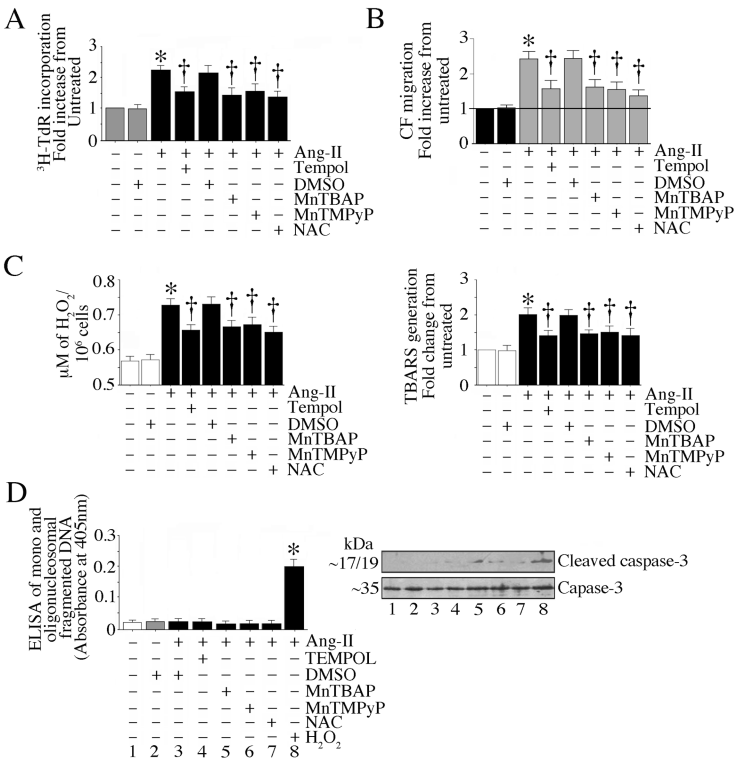


**Fig. 2. Oxidative stress contributes to Ang-II-induced CF proliferation and migration**

A, The SOD mimetics attenuate Ang-II-induced CF proliferation. The quiescent CF were incubated with NAC (5mM in water for 30 min), Tempol (1 μM in DMSO), MnTBAP (100 μM in water) or MnTMPyP (1 μM in water) for 30 min prior to Ang-II ($10^{-7}$M) addition. Proliferation was analyzed after 48 h. B, The antioxidant NAC and the SOD mimetics attenuate Ang-II-induced CF migration. The quiescent CF were layered on Matrigel™ basement membrane matrix-coated filters, and then treated with NAC, Tempol, MnTBAP or MnTMPyP as in A prior to Ang-II ($10^{-7}$M) addition. After 12 h, cells migrating to the other side of the membrane were quantified using the MTT assay. C, The antioxidant NAC and the SOD mimetics inhibit Ang-II-induced $H_2O_2$ production and lipid peroxidation. The quiescent CF treated as in A, but for 30 min ($H_2O_2$ production) or 2 h (TBARS) with Ang-II ($10^{-7}$M) were analyzed for $H_2O_2$ production using the Amplex® Red Hydrogen Peroxide/ Peroxidase Assay Kit. Lipid peroxidation was analyzed using the TBARS Assay kit. D, The antioxidant NAC and the SOD mimetics did not induce cell death. CF treated as in A were analyzed for mono and oligonucleosomal fragmented DNA in cytoplasmic extracts using a cell death ELISA. Total (~35 kDa) and cleaved (active form; p17/19) caspase-3 levels at 8 h were analyzed by immunoblotting using cleared whole cell lysates (n=3). A–D, * at least $P < 0.01$ vs. untreated, †$P <$ at least 0.05 vs. Ang-II (n = 12).

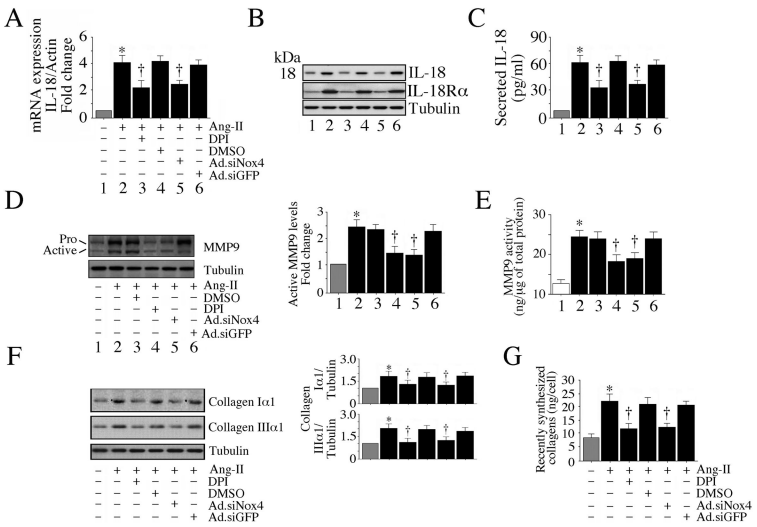


**Fig. 3. Ang-II induces IL-18 and MMP9 expression via Nox4 and ROS**

*A*, *B*, *C*, Ang-II induces IL-18 and IL-18Rα expression and IL-18 secretion. CF infected with Ad.siNox4 (MOI 100 for 24 h) or treated with DPI (10 μM for 30 min) prior to Ang-II ($10^{-7}$M) treatment for 2 (*A*, *B*) or 24 h (*C*) were analyzed for IL-18 mRNA expression by RT-qPCR (*A*, n=6), mature IL-18 (18 kDa form) and IL-18Rα protein levels in cleared whole cell lysates by immunoblotting (n=3), and secreted IL-18 levels in equal amounts of culture supernatants by ELISA (n=6). *D*, *E*, Ang-II induces MMP9 activation. The CF made quiescent in RPMI 1640 medium supplemented with ITS were treated with Ang-II ($10^{-7}$M) for 2 (*D*) or 24 h (*E*). The culture supernatant was concentrated and 1μg/sample was analyzed by immunoblotting using antibodies that detect both pro and active forms of MMP9 (D). Densitometric analysis of the immunoreactibe bands from three independent experiments is summarized on the right. Enzymatic activity was also analyzed by a Biotrak activity assay kit (E). E, $*P < 0.01$ *vs.* respective untreated; $\dagger P <$ at least 0.05 *vs.* Ang-II ± Ad.siGFP or DMSO (n=6). F, G. Ang-II increases collagen expression. The quiescent CF were treated with Ang-II ($10^{-7}$M) for 2 (*F*) or 72 h (*G*), and analyzed for collagens I and III by immunoblotting (F; n=3). Levels of soluble collagens released into culture media at 72 h were determined by Sircol™ collagen assay (G). *A*, *C*, $*P < 0.001$ *vs.* untreated. A–G, $*P <$ at least 0.05 *vs.* respective untreated, $\dagger P <$ at least 0.05 *vs.* Ang-II (n=3–6).

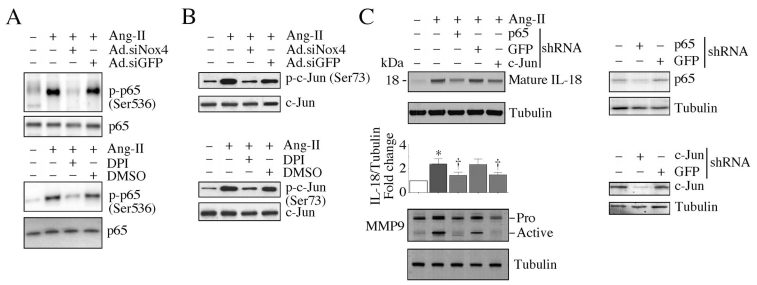


**Fig. 4. Ang-II stimulates IL-18 and MMP9 expression via Nox4/ROS-dependent NF-κB and AP-1 activation**

A, Ang-II stimulates NF-κB/p65 activation via Nox4 and ROS. The quiescent CF were treated with DPI (10 μM in DMSO for 30 min) prior to Ang-II ($10^{-7}$M for 30 min) addition. Phospho-p65 levels were analyzed by immunoblotting using cleared whole cell homogenates and activation-specific antibodies (upper and lower panels; n=3). B, Ang-II stimulates AP-1/c-Jun activation via Nox4 and ROS. The quiescent CF treated as in A were analyzed for phospho-c-Jun levels by immunoblotting using cleared whole cell homogenates and activation-specific antibodies (upper and lower panels; n=3). C, Ang-II induced IL-18 expression and MMP9 activation via NF-κB and AP-1. CF were infected with lentiviral p65 or c-Jun shRNA (MOI0.5) for 48 h. In the last 24 h, the complete media was replace with 0.5% BSA (IL-18) or RPMI 1640/ITS medium (MMP9), and then treated with Ang-II for 2 (IL-18) or 24 h (MMP9). IL-18 expression was analyzed by immunoblotting (n=3) using cleared whole cell lysates and antibodies that specifically detect the mature form (upper panel). MMP9 activity was analyzed using 1 μg of protein concentrated from culture supernatants (lower panel; n=3). Knockdown of p65 and c-Jun was confirmed by immunoblotting (right panels; n=3).

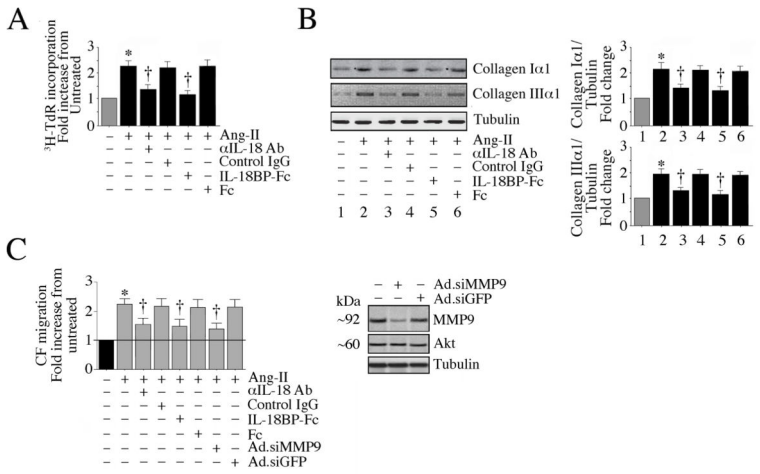


**Fig. 5. Ang-II stimulates CF proliferation and migration via IL-18 and MMP9**

*A*, Ang-II stimulates CF proliferation via IL-18. The quiescent CF were incubated with IL-18 neutralizing antibodies or IL-18BP-Fc chimera (10 μg/ml for 1 h) prior to Ang-II addition ($10^{-7}$M for 48 h). Control IgG or Fc alone served as controls. Cell proliferation was analyzed as in Fig. 1A. B, Ang-II induces collagen expression via IL-18. CF treated as in A, but for 3 h with Ang-II, were analyzed for collagens Iα1 and IIIα1 expression by immunoblotting. Densitometric analysis of the immunoreactive bands from three independent experiments is summarized on the right. C, Ang-II stimulates CF migration via IL-18 and MMP9. CF layered on Matrigel™ basement membrane matrix-coated filters were incubated with IL-18 neutralizing antibodies or IL-18BP-Fc chimera (10 μg/ml) for 1 h followed by Ang-II ($10^{-7}$M) for 12 h. Cell migration was analyzed as in Fig. 1B. Studies were also performed by layering CF infected with Ad.siMMP9 (MOI100 for 24 h) on Matrigel™ and then treated with Ang-II for 12 h. Knockdown of MMP9 was confirmed by immunoblotting (right hand panel, n=3). A–C, *$P <$ at least 0.05 *vs.* respective untreated; †$P <$ at least 0.05 *vs.* Ang-II ± Control IgG or Ad.siGFP (n=12).

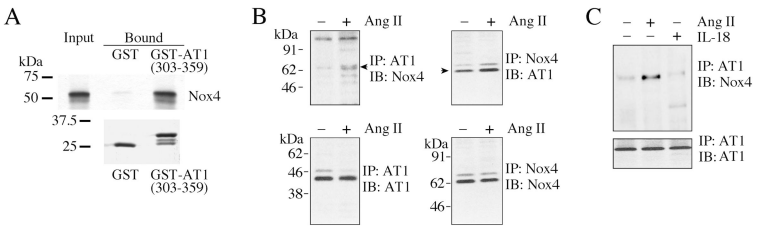


**Fig. 6. Ang-II increases the physical association of AT1 and Nox4 *in vitro and in vivo***

*A*, Nox4 binds the C-terminal domain of AT1 *in vitro*. A pull-down assay was carried out between a protein composed of the C-terminal cytoplasmic domain of AT1 fused to GST (GST-AT1(303-359)), pre-bound to GSH-sepharose beads, and *in vitro* transcribed/translated, $^{35}$S-methionine labeled mouse Nox4 ([$^{35}$S]Met-Nox4). GST was used as a binding specificity control. Upper panel, aliquots of labeled Nox4 added to GST or GST-AT1(303-359) (equivalent to 2% of the total, "Input"), and the bound Nox4 eluted with SDS-PAGE treatment buffer from the GSH-sepharose beads after washing. Eluates (equivalent to 10% of eluate, "Bound") were analyzed by SDS-PAGE and fluorography. Lower panel, to show the equal loading of the GSH-sepharose beads with GST and GST-AT1(303-359), equal volumes of the eluates were analyzed by SDS-PAGE and stained for protein with GelCode™ Blue Stain Reagent. *B*, AT1 and Nox4 association *in vivo* is increased by Ang-II. The quiescent CF were treated with or without Ang-II ($10^{-7}$ M for 15 min), and AT1 and Nox4 binding was analyzed by co-immunoprecipitation/immunoblotting (co-IP/IB) using cleared cell lysates (left and *right*). All blots are representatives from three independent experiments. *C,* IL-18 fails to modulate AT1 binding to Nox4. The quiescent CF were treated with IL-18 (1 ng/ml for 15 min). Ang-II served as a positive control. Cell lysates were analyzed for AT1/Nox4 binding by co-IP/IB (left and right; $n = 3$).

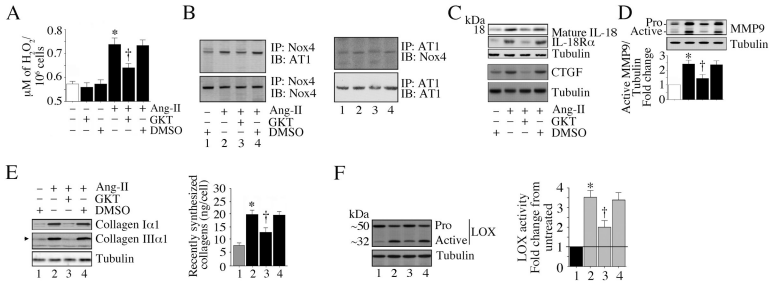


**Fig. 7. The Nox1/Nox4 dual inhibitor GKT137831 inhibits AT1/Nox4 binding and Ang-II-induced IL-18 and MMP9 expression**

A, GKT137831 (GKT) inhibits Ang-II-induced $H_2O_2$ production. The quiescent CF were incubated with GKT (5 μM for 15 min) prior to Ang-II addition ($10^{-7}$M for 30 min). $H_2O_2$ levels were quantified using the Amplex® Red Hydrogen Peroxide/Peroxidase Assay Kit. B, GKT inhibits AT1/Nox4 binding. The quiescent CF were treated with GKT (5 μM for 15 min) prior to Ang-II addition ($10^{-7}$ M for 15 min). AT1 and Nox4 binding was analyzed by co-IP/IB using cleared cell lysates (left and *right*). All blots are representatives from three independent experiments. C, GKT inhibits Ang-II-induced IL-18, IL-18Rα, and CTGF expression. The quiescent CF were treated with GKT for 15 min followed by Ang-II for 2 h. IL-18, IL-18Rα, and CTGF expression levels were analyzed by immunoblotting (n=3). D, GKT inhibits Ang-II-induced MMP-9 activation. CF made quiescent in RPMI/ITS medium were treated with GKT for 15 min followed by Ang-II for 2 h. MMP9 activation was analyzed by immunoblotting using cleared whole cell homogenates. Densitometric analysis of immunoreactive bands representing active MMP9 were semiquantified and results from three independent experiments are summarized in the bottom. E, GKT inhibits Ang-II-induced collagen expression and secretion. CF treated as in C, but for 2 h (immunoblotting) or 72 h (secretion) with Ang-II were analyzed by immunoblotting (left hand panel, n=3). Secreted collagens were analyzed by Sircol™ Collagen assay (right hand panel). F, GKT attenuates Ang-II-induced LOX activation. The quiescent CF treated as in C, but for 2 h (protein levels) or 72 h (secreted collagens) with Ang-II were analyzed by immunoblotting (left hand panel; n=3). Secreted collagens were analyzed by Sircol™ Collagen assay (right hand panel). F, GKT inhibits Ang-II-induced LOX activation. The quiescent CF were treated with GKT prior to Ang-II addition ($10^{-7}$M, 24 h). LOX activity was analyzed by immunoblotting using antibodies that detect both pro and active forms (left hand panel, n=3). LOX activity was also analyzed using the conditioned medium and diaminopentane as a substrate and Amplex red as a $H_2O_2$ probe (n = 6). A, C, E, F, *$P$ < at least 0.05 *vs.* untreated; †$P$ < at least 0.05 *vs.* Ang-II (n=3–6).

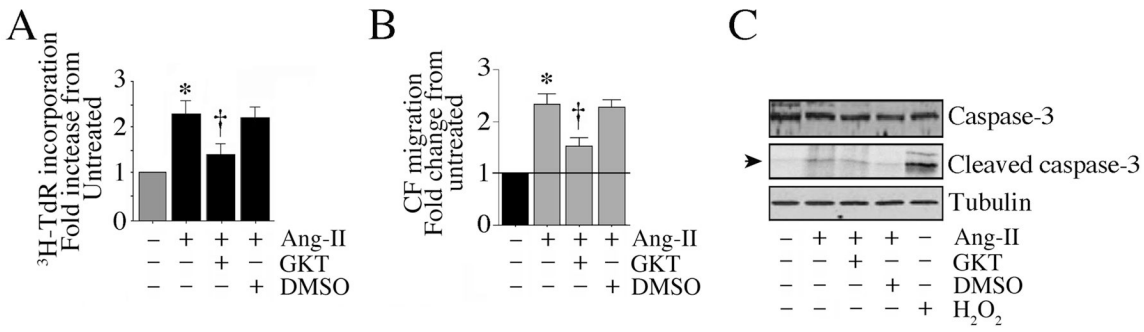


**Fig. 8. GKT137831 inhibits Ang-II-induced cardiac fibroblast proliferation and migration**

A, GKT attenuates Ang-II-induced CF proliferation. The quiescent CF were treated with GKT (5 μM for 15 min) prior to Ang-II addition ($10^{-7}$M for 48 h). CF proliferation was analyzed as in Fig. 1A. B, GKT attenuates Ang-II-induced CF migration. The quiescent CF were layered on Matrigel™ basement membrane matrix-coated filters, and then treated with GKT (5 μM for 15 min) prior to Ang-II addition ($10^{-7}$M for 12 h). Cell migration was analyzed as in Fig. 1B. C, GKT does not induce cell death. CF treated as in A, but for 8 h, were analyzed for total and cleaved (active form) caspase-3 levels by immunoblotting (n=3). $H_2O_2$ (100 μM) served as a positive control. A, B, *$P$ < 0.001 *vs.* untreated, †$P$ < at least 0.01 *vs.* Ang-II (n = 12).

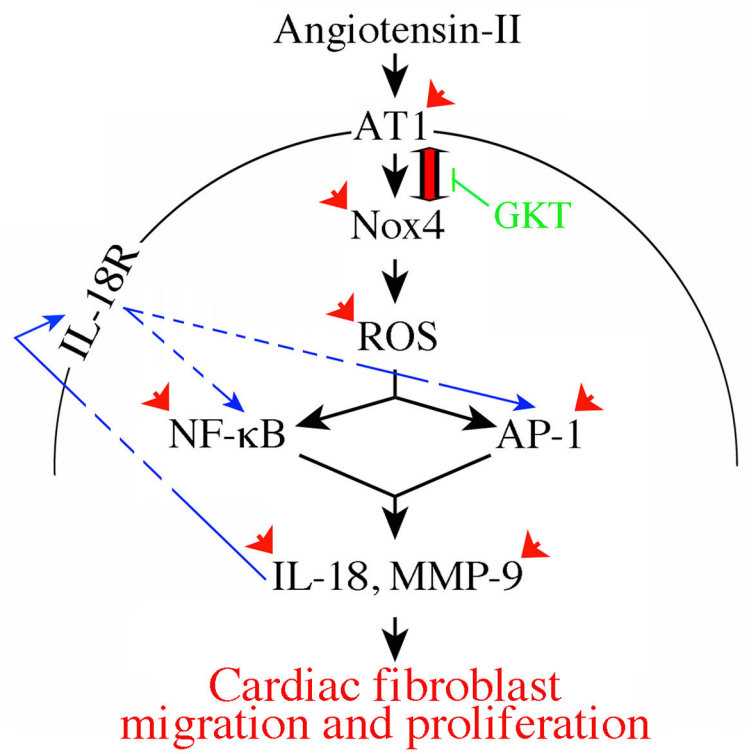


**Fig. 9. Schema showing the possible signal transduction pathways involved in Ang-II induced CF proliferation and migration**

Double arrow denotes AT1/Nox4 physical association. Arrowheads denote interventions used in delineating the signaling pathway. Arrows in blue show amplification in IL-18's pro-mitogenic and pro-migratory effects in cardiac fibroblasts. The Nox1/Nox4 dual inhibitor GKT137831 attenuates not only AT1/Nox4 interaction, but also Ang-II-induced proinflammatory, pro-mitogenic and pro-migratory effects.